

In-medium Properties of Hadrons – Observables

T. Falter, J. Lehr, U. Mosel, P. Muehlich, M. Post
Institut fuer Theoretische Physik, Universitaet Giessen
D-35392 Giessen, Germany

November 15, 2018

Abstract

We first briefly review the theoretical basis for calculations of changes of hadronic properties in dense nuclear matter. These changes have usually been investigated by means of relativistic heavy-ion reactions. Here we discuss that observable consequences of such changes can also be seen in more elementary reactions on nuclei. Particular emphasis is put on a discussion of actual observables in photonuclear reactions; we discuss in detail η - and vector-meson production. We show that photoproduction of η 's can yield essential information on in-medium properties of the $S_{11}(1535)$ resonance while the ϕ meson properties will probably not be accessible through the K^+K^- decay channel. However, for ω mesons the $\pi^0\gamma$ decay channel, due to its reduced final state interaction, looks more promising in this respect. Completely free of final state interactions is dilepton production in the few GeV range. We show that the sensitivity of this decay channel to changes of hadronic properties in medium in photonuclear reactions on nuclei is as large as in ultrarelativistic heavy ion collisions. Finally we discuss that hadron production in nuclei at 10 – 20 GeV photon energies can give important information on the hadronization process.

1 Introduction

That hadrons can change their properties and couplings in the nuclear medium has been well known to nuclear physicists since the days of the Delta-hole model that dealt with the changes of the properties of the pion and Delta-resonance inside nuclei [1]. Due to the predominant p -wave interaction of pions with nucleons one observes here a lowering of the pion branch for small but finite pion momenta, which increases with the nucleon-density. More recently, experiments at the FSR at GSI have shown that also the pion rest mass in medium differs from its value in vacuum [2]. This is interesting since there are also recent experiments [3] that look for the in-medium changes of the σ meson, the chiral partner of the pion. Any comparison of scalar and pseudoscalar strength could thus give information about the degree of chiral symmetry restoration in nuclear matter.

In addition, experiments for charged kaon production at GSI [4] have given some evidence for the theoretically predicted lowering of the K^- mass in medium and the (weaker) rising of the K^+ mass. State-of-the-art calculations of the in-medium properties of kaons have shown that the usual quasi-particle approximation for these particles is no longer justified inside nuclear matter where they acquire a broad spectral function [5, 6].

At higher energies, at the CERN SPS and most recently at the Brookhaven RHIC, in-medium changes of vector mesons have found increased interest, mainly because these mesons couple strongly to the photon so that electromagnetic signals could yield information about properties of hadrons deeply embedded into nuclear matter. Indeed, the CERES experiment [7] has found a considerable excess of dileptons in an invariant mass range from ≈ 300 MeV to ≈ 700 MeV as compared to expectations based on the assumption of freely radiating mesons. This result has found an explanation in terms of a shift of the ρ meson spectral function down to lower masses, as expected from theory (see, e.g., [8, 9, 10, 11]). However, the actual reason for the observed dilepton excess is far from clear. Both models that just shift the pole mass of the vector meson as well as those that also modify the spectral shape have successfully explained the data [12, 13, 14]; in addition, even a calculation that just used the free radiation rates with their – often quite large – experimental uncertainties was compatible with the observations [15]. There are also calculations that attribute the observed effect to radiation from a quark-gluon plasma [16]. While all these quite different model calculations tend to explain the data, though often with some model assumptions, their

theoretical input is sufficiently different as to make the inverse conclusion that the data prove one or another of these scenarios impossible.

One of the authors has, therefore, already some years ago proposed to look for the theoretically predicted changes of vector meson properties inside the nuclear medium in reactions on normal nuclei with more microscopic probes [17, 18]. Of course, the nuclear density felt by the vector mesons in such experiments lies much below the equilibrium density of nuclear matter, ρ_0 , so that naively any density-dependent effects are expected to be much smaller than in heavy-ion reactions.

On the other hand, there is a big advantage to these experiments: they proceed with the spectator matter being close to its equilibrium state. This is essential because all theoretical predictions of in-medium properties of hadrons are based on a model in which the hadron (vector meson) under investigation is embedded in cold nuclear matter in equilibrium and with infinite extension. However, a relativistic heavy-ion reaction proceeds – at least initially – far from equilibrium. Even if equilibrium is reached in a heavy-ion collision this state changes by cooling through expansion and particle emission and any observed signal is built up by integrating over the emissions from all these different stages of the reaction.

Another in-medium effect arises when particles are produced by high-energy projectiles inside a nuclear medium. A major experimental effort at RHIC experiments has gone into the observation of jets in ultra-relativistic heavy-ion collisions and the determination of their interaction with the surrounding quark or hadronic matter [19]. A complementary process is given by the latest HERMES results at HERA for high-energy electroproduction of hadrons off nuclei [20]. Again, the advantage of the latter experiment is that the nuclear matter with which the interactions happen is at rest and in equilibrium.

In this lecture note we summarize results that we have obtained in studies of observable consequences of in-medium changes of hadronic spectral functions as well as hadron formation in reactions of elementary probes with nuclei. We demonstrate that the expected in-medium sensitivity in such reactions is as high as that in relativistic heavy-ion collisions and that in particular photonuclear reactions present an independent, cleaner testing ground for assumptions made in analyzing heavy-ion reactions.

2 Theory

A large part of the current interest in in-medium properties of hadrons comes from the hope to learn something about quarks in nuclei. Indeed, a very simple estimate shows that the chiral condensate in the nuclear medium is in lowest order in density given by [11]

$$\langle \bar{q}q \rangle_{\text{med}}(\rho, T) \approx \left(1 - \sum_h \frac{\Sigma_h \rho_h^s(\rho, T)}{f_\pi^2 m_\pi^2} \right) \langle \bar{q}q \rangle_{\text{vac}} . \quad (1)$$

Here ρ_s is the *scalar* density of the hadron h in the nuclear system and Σ_h the so-called sigma-commutator that contains information on the chiral properties of h . The sum runs over all hadronic states. While (1) is nearly exact, its actual applicability is limited because neither the sigma-commutators of the higher lying hadrons nor their scalar densities are known. However, at very low temperatures close to the groundstate these are accessible. Here $\rho_s \approx \rho_v \frac{m}{E}$ so that the condensate drops linearly with the nuclear (vector) density. This drop can be understood in physical terms: with increasing density the hadrons with a chirally symmetric phase in their interior fill in more and more space in the vacuum with its spontaneously broken chiral symmetry. Note that this is a pure volume effect; it is there already for a free, non-interacting hadron gas.

How this drop of the scalar condensate translates into observable hadron masses is not uniquely prescribed. The only rigorous connection is given by the QCD sum rules that relates an integral over the hadronic spectral function to a sum over combinations of quark- and gluon-condensates with powers of $1/Q^2$. The starting point for this connection is the current-current correlator

$$\Pi_{\mu\nu}(q) = i \int d^4x e^{iqx} \langle T j_\mu(x) j_\nu(0) \rangle , \quad (2)$$

where the current is expressed in terms of quark-field operators. This correlator can be decomposed [21]

$$\Pi_{\mu\nu}(q) = q_\mu q_\nu R(q^2) - g_{\mu\nu} \Pi^{\text{isotr}}(q^2) . \quad (3)$$

The QCD sum rule then reads

$$R^{\text{OPE}}(Q^2) = \frac{\tilde{c}_1}{Q^2} + \tilde{c}_2 - \frac{Q^2}{\pi} \int_0^\infty ds \frac{\text{Im} R^{\text{HAD}}(s)}{(s + Q^2)s} \quad (4)$$

with $Q^2 := -q^2 \gg 0$ and some subtraction constants \tilde{c}_i . Here R^{OPE} represents a Wilson's operator expansion of the current-current correlator in terms of quark and gluon degrees of freedom in the space-like region. On the other hand, $R^{\text{HAD}}(s)$ in (4) is the same object for time-like momenta, represented by a parametrization in terms of hadronic variables. The dispersion integral connects time- and space-like momenta. Eq. (4) also connects the hadronic with the quark world. It allows – after the technical step of a Borel transformation – to determine parameters in a hadronic parametrization of $R^{\text{HAD}}(s)$ by comparing the lhs of this equation with its rhs.

The operator product expansion of R^{OPE} on the lhs involves quark- and gluon condensates [21, 22]; of these only the two-quark condensates are reasonably well known, whereas our knowledge about already the four-quark condensates is rather sketchy.

Leupold et al. [21, 22] have shown that using a realistic parametrization of the hadronic spectral function on the rhs of (4)

$$\text{Im}R^{\text{HAD}}(s) = \Theta(s_0 - s)\text{Im}R^{\text{RES}}(s) + \Theta(s - s_0)\frac{1}{8\pi}\left(1 + \frac{\alpha_s}{\pi}\right) \quad (5)$$

where s_0 denotes the threshold between the low energy region described by a spectral function for the lowest lying resonance, $\text{Im}R^{\text{RES}}$, and the high energy region described by a continuum calculated from perturbative QCD. The second term on the rhs of (5) represents the QCD perturbative result that survives when $s \rightarrow \infty$. Using the measured, known vacuum spectral function for R^{HAD} allows one to obtain information about the condensates appearing on the lhs of (4). On the other hand, modelling the density-dependence of the condensates yields information on the change of the hadronic spectral function when the hadron is embedded in nuclear matter. Since the spectral function appears under an integral the information obtained is not very precise. However, Leupold et al. have shown [21, 22] that the QCDSR provides important constraints for the hadronic spectral functions in medium, but it does not fix them. Recently Kaempfer et al have turned this argument around by pointing out that measuring an in-medium spectral function of the ω meson could help to determine the density dependence of the higher-order condensates [23].

Thus models are needed for the hadronic interactions. The quantitatively reliable ones can at present be based only on 'classical' hadrons and their interactions. Indeed, in lowest order in the density the mass and width of an interacting hadron in nuclear matter at zero temperature and vector density

ρ_v are given by (for a meson, for example)

$$\begin{aligned} m^{*2} &= m^2 - 4\pi\Re f_{mN}(q_0, \theta = 0) \rho_v \\ m^*\Gamma^* &= m\Gamma^0 - 4\pi\Im f_{mN}(q_0, \theta = 0) \rho_v . \end{aligned} \quad (6)$$

Here $f_{mN}(q_0, \theta = 0)$ is the forward scattering amplitude for a meson with energy q_0 on a nucleon. The width Γ^0 denotes the free decay width of the particle. For the imaginary part this is nothing other than the classical relation $\Gamma^* - \Gamma^0 = v\sigma\rho_v$ for the collision width, where σ is the total cross section. This can easily be seen by using the optical theorem.

Note that such a picture also encompasses the change of the chiral condensate in (1), obtained there for non-interacting hadrons. If the spectral function of a non-interacting hadron changes as a function of density, then in a classical hadronic theory, which works with fixed (free) hadron masses, this change will show up as an energy-dependent interaction and is thus contained in any empirical phenomenological cross section.

Unfortunately it is not a-priori known up to which densities the low-density expansion (6) is useful. Post et al. have recently investigated this question in a coupled-channel calculation of selfenergies [10]. Their analysis comprises pions, η -mesons and ρ -mesons as well as all baryon resonances with a sizeable coupling to any of these mesons. Fig. 1 shows a typical selfenergy graph in their calculation. Of particular importance are the $\Delta(1232)$, the $S_{11}(1535)$ and the $D_{13}(1520)$ resonances for the pion, the η -meson and the ρ -meson, respectively.

The authors of [10] find that already for densities less than $0.5\rho_0$ the linear scaling of the selfenergies inherent in (6) is badly violated for the ρ and the π mesons, whereas it is a reasonable approximation for the η meson, but even in the latter case already at $0.5\rho_0$ the selfenergy does not scale exactly with ρ . Reasons for this deviation from linearity are Fermi-motion, Pauli-blocking, selfconsistency and short-range correlations. For different mesons different sources of the discrepancy prevail: for the ρ and η mesons the iterations act against the low-density theorem by inducing a strong broadening for the $D_{13}(1520)$ and a slightly repulsive mass shift for the $S_{11}(1535)$ nucleon resonances to which the ρ and the η meson, respectively, couple. The effects of self-consistency on the spectral function of the ρ -meson can nicely be seen in Fig. 2. The figure shows that the spectral function of a ρ meson at rest in the nuclear medium (upper left, solid curve) exhibits a remarkable structure that is generated by the strong coupling to the $D_{13}(1520)$ resonance. While this

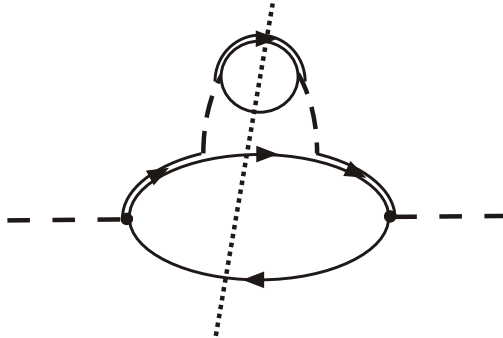


Figure 1: Selfenergy diagram for a meson coupling to an in-medium resonance. The dotted line shows a possible cut through the diagram to generate the imaginary part of the selfenergy (from [10]). Here a nucleon is represented by a solid line, a meson by a dashed line and a baryon resonance by a double line.

structure disappears at the highest momentum considered here, the spectral function for the transverse vector meson (lower left) is still considerably different from that of a ρ in vacuum. Notice also that the longitudinal spectral function (right column) retains more of the original vector meson structure.

3 Particle Production on Nuclei – Observables

Traditionally, heavy-ion reactions are assumed to be the reactions of choice for an investigation of in-medium properties. After all, here very high nuclear densities ($2-10\rho_0$) can be reached with present day's accelerators so that any density-dependent effect would be magnified. However, any explanations of observed effects always suffer from an inherent inconsistency: The observed signal, on one hand, necessarily integrates over many different stages of the collision – nonequilibrium and equilibrium, the latter at various densities and temperatures. On the other hand, the theoretical input is always calculated under the simplifying assumption of a hadron in nuclear matter in equilibrium. We have therefore looked for possible effects in reactions that proceed

much closer to equilibrium, i.e. reactions of elementary probes such as protons, pions, and photons on nuclei. Of course, the densities probed in such reactions are always $\leq \rho_0$, with most of the nucleons actually being at about $0.5\rho_0$. On the other hand, the target is obviously stationary and the reaction proceeds much closer to (cold) equilibrium than in a relativistic heavy-ion collision.

It is thus a quantitative question if any observable effects of in-medium changes of hadronic properties survive if the densities probed are always $\leq \rho_0$. With the aim of answering this question we have over the last few years undertaken a number of calculations for proton- [24], pion- [44, ?] and photon- [26] induced reactions. All of them have one feature in common: they treat the final state incoherently in a coupled channel transport calculation that allows for elastic and inelastic scattering of, particle production by and absorption of the produced hadrons (vector mesons). A new feature of these calculations is that vector mesons with their correct spectral functions can actually be produced and transported consistently. This is quite an advantage over earlier treatments [27] in which the mesons were always produced and transported with their pole mass and their spectral function was later on folded in only for their decay.

In all photonuclear calculations above energies of about 1 GeV we account for coherent initial state interactions of the incoming photon which lead to shadowing. In an interaction with a bound nucleon the shadowed incoming photon then produces a hadronic final state which cascades through the nucleus [28, 29]. The incoherent final state interactions are treated as just described by means of a semi-classical coupled-channel transport theory. For details of the model see Ref. [26] and references therein.

3.1 η Production

We first look at the prospects of using reactions with hadronic final states and discuss the photo-production of η -mesons on nuclei as a first example. These mesons are unique in that they are sensitive to one dominating resonance only (the $S_{11}(1535)$) so that one may hope to learn something about the properties of this resonance inside nuclei. Experiments for this reaction were performed both by the TAPS collaboration [30] and – for higher energies – at KEK [31].

Estimates of the collisional broadening of the $S_{11}(1535)$ resonance have given a collision width of about 35 MeV at ρ_0 [32]. The more recent, and

more refined, selfconsistent calculations of [10] give a very similar value for this resonance. In addition, a dispersive calculation of the real part of the selfenergy for the resonance at rest gives only an insignificant shift of the resonance position. Thus any momentum-dependence of the selfenergy as observed in photon-nucleus data can directly be attributed to binding energy effects [33].

The results of this calculation [33] are shown in Fig. 3. The dashed line in Fig. 3 gives the results of a calculation employing a momentum-independent potential for the $S_{11}(1535)$ resonance with the same depth at ρ_0 as for the nucleons. It is clearly seen that it rises too steeply and peaks at a too low energy compared to the data. The solid line, that describes all available data over a wide energy range very well, employs a momentum-dependence in the nucleon and resonance potentials taken from earlier fits to heavy-ion reaction data. For the present discussion the relevant feature of this potential is that it vanishes for momenta around 800 MeV. Thus, for photon energies around this values, close to the peak position in the data, the resonance is no longer bound whereas the hit nucleon is bound by about 75 MeV at ρ_0 . Thus, effectively the resonance is shifted upwards by this amount; this is just what the data show. In addition, Fig. 3 also contains a dotted line, exhibiting the effects of the in-medium width of the $S_{11}(1535)$ resonance. Since the latter is small, also its effect on the eta-production cross section is small.

3.2 ϕ Production

As a second example we look into the photoproduction of ϕ -mesons in nuclei. Our calculations of this reaction have been motivated by the idea to learn about the ϕ in-medium properties by measuring the K^+K^- mass distribution [34]. It has been proposed to perform such an experiment at the Spring8 facility in Osaka [35]. In principle the ϕ meson forms a unique probe since it is the only resonance decaying into K^+K^- pairs in the considered mass region. Theoretical approaches to the ϕ in-medium properties find a broadening of the ϕ meson of up to 40 MeV at nuclear matter density and vanishing ϕ momentum [36]. While this value exceeds the vacuum value of 4.4 MeV by about one order of magnitude, a possible mass shift of the ϕ is expected to be of the order of only -10 MeV to -30 MeV [37] so that the ϕ meson is expected to survive as a proper quasiparticle even at nuclear matter density ρ_0 [38]. Thus the expected modification might lead to observable consequences because of the small width of the ϕ meson.

Only vector mesons decaying inside the nucleus may reveal informations about their in-medium properties. Hence, the decay length of these vector mesons $L_V = p_V/(m_V\Gamma_V)$ has to be of the order of the nuclear radius. In order to produce ϕ mesons with the required low momenta in the target rest frame the incident photon energy has to be chosen not too close above threshold (~ 1.5 GeV). Simulations at higher photon energies require to include also inclusive photoproduction processes. This is illustrated in Fig. 4, which shows the momentum distribution of ϕ mesons with (solid line) and without FSI (dashed) from a nuclear target (^{40}Ca). It is clearly seen that the cross section at small ϕ momenta is dominated by the inclusive production processes. In the simulations inclusive photoproduction of vector mesons has been accounted for by means of the hadronic event generator FRITIOF employing the vector meson dominance model in order to describe the photon-hadron coupling [34]. Also visible from Fig. 4 is the fact, that the FSI of the ϕ , through their non-absorptive part, produce an accumulation of ϕ mesons in the low-momentum part of the spectrum. The number of ϕ mesons decaying in the medium is greatly enhanced by this effect.

Including collisional broadening by means of the low-density expansion (6) and applying a rather severe momentum cutoff to the three momentum of the detected K^+K^- pair, we find an observable broadening of the invariant mass spectrum by almost a factor of two, see Fig. 5. However, accounting also for the electromagnetic potential which already in ^{40}Ca has a depth of 11 MeV, the average decay density of reconstructed ϕ mesons decreases considerably. As a consequence the obtained invariant mass spectrum again is very close to the free one (dotted in Fig. 5). Also the dropping ϕ mass (30 MeV at ρ_0 in the simulation) has no remarkable effect, since as long as the K^+ and K^- properties are not changed in the medium ϕ mesons with considerably reduced masses do not decay into K^+K^- pairs. This also leads to a reduced average decay density.

As already mentioned, also the kaon properties receive a rather dramatic change in the nuclear environment [39]. Kaons from ϕ decays that propagate through a potential gradient change their momenta and, hence, also the invariant mass of any K^+K^- pair. This effect leads to an accumulation of strength on the high mass side of the invariant mass spectrum, see Fig. 6. In summary, we find, that due to the medium modification of the ϕ decay products (the kaons) one cannot learn anything about the ϕ properties in the $A(\gamma, K^+K^-)X$ reaction, but rather about the existence of an in-medium change of the K^+ and K^- mesons.

3.3 ω Production

In contrast to the results for the ϕ meson, the situation looks more promising for the ω meson [40]. On the one hand, the ω is much lighter than the ϕ and can, therefore, be produced with lower momentum inside nuclei. On the other hand, the $\pi^0\gamma$ decay mode is not influenced by the electromagnetic potential and also FSI effects might be less pronounced because of the weak photon-nucleon coupling. An experiment measuring the $A(\gamma, \pi^0\gamma')X$ reaction is presently being analyzed by the TAPS/Crystal Barrel collaborations at ELSA [41]. The varying theoretical predictions for the ω mass (640-765 MeV) [42] and width (up to 50 MeV) [43, 44] in nuclear matter at rest encourage the use of such an exclusive probe to learn about the ω spectral distribution in nuclei.

Simulations have been performed at 1.2 GeV and 2.5 GeV photon energy, which cover the accessible energies of the TAPS/Crystal Barrel experiment. After reducing the combinatorial and rescattering background by applying kinematic cuts on the outgoing particles, we obtain rather clear signals for a dropping ω mass inside nuclei. The solid line in Fig. 7 shows results of a calculation including both collisional broadening and a lowering of the ω mass. It exhibits a shoulder on the low-mass side of the peak and a clear excess there over the proton distribution, also shown in the figure. This has to be compared to the dashed line, which includes collisional broadening only. Therefore, in this particular case it is possible to disentangle rather trivial in-medium changes (collisional broadening) from more interesting medium-modifications (dropping mass), which may be related to a change of the chiral condensate at finite nuclear density [45].

Employing the low-density expansion of Eq. (6) to determine the effective in-medium mass of the ω one obtains a momentum dependence which is driven by the energy dependence of the ω -nucleon total cross section. Such a simple-minded approach yields a considerably reduced mass for ω mesons at rest and a fast increase of the effective mass for ω mesons moving with finite velocity, arriving rather fast at values close to the ω vacuum mass [40]. The results of simulations adopting this momentum dependent mass are also shown in Fig. 7 (dash-dotted line). As expected the results of these calculations are again very similar to the results obtained without any real ω potential. Measurements with varying momentum cuts may help to disentangle the density and momentum dependence of the in-medium self-energy of the ω meson.

3.4 Dilepton Production

Dileptons, i.e. electron-positron pairs, in the outgoing channel are an ideal probe for in-medium properties of hadrons since they – in contrast to hadronic probes – experience no strong final state interaction. A first experiment to look for these dileptons in heavy-ion reactions was the DLS experiment at the BEVALAC in Berkeley [46]. Later on, and in a higher energy regime, the CERES experiment has received a lot of attention for its observation of an excess of dileptons with invariant masses below those of the lightest vector mesons [7]. Explanations of this excess have focused on a change of in-medium properties of these vector mesons in dense nuclear matter (see e.g. [12, 13]). The radiating sources can be nicely seen in Fig. 8 that shows the dilepton spectrum obtained in a low-energy run at 40 AGeV together with the elementary sources of dilepton radiation.

The figure exhibits clearly the rather strong contributions of the vector mesons – both direct and through their Dalitz decay – at invariant masses above about 500 MeV. If this strength is shifted downward, caused by an in-medium change of the vector-meson spectral functions, then the observed excess can be explained as has been shown by various authors (see e.g. [27] for a review of such calculations). The results of a new calculation, based on the spectral function in Fig. 2, are shown in Fig. 9. The strong amplification of the dilepton rate at small invariant masses is caused by the photon propagator, which contributes $\sim 1/q^4$ to the cross section. Any strength in the spectral function at finite density at small q^2 is thus dramatically amplified.

In view of the uncertainties in interpreting these results discussed earlier we have studied the dilepton production in reactions on nuclear targets involving more elementary projectiles. It is not *a priori* hopeless to look for in-medium effects on dilepton production in ordinary nuclei: Even in relativistic heavy-ion reactions that reach baryonic densities of the order of 3 - 10 ρ_0 many observed dileptons actually stem from densities that are much lower than these high peak densities. Transport simulations have shown [27] that even at the CERES energies about 1/2 of all dileptons come from densities lower than $2\rho_0$. This is so because in such reactions the pion-density gets quite large in particular in the late stages of the collision, where the baryonic matter expands and its density becomes low again. Correspondingly many vector mesons are formed (through $\pi + \pi \rightarrow \rho$) late in the collision and their decay to dileptons thus happens at low baryon densities.

A typical result of such a calculation for the dilepton yield – after remov-

ing the Bethe-Heitler component – is given in Fig. 10. Comparing this figure with Fig. 8 shows that in a photon-induced reaction at 1 - 2 GeV photon energy exactly the same sources, and none less, contribute to the dilepton yield as in relativistic heavy-ion collisions at 40 AGeV! The question now remains if we can expect any observable effect of possible in-medium changes of the vector meson spectral functions in medium in such an experiment on the nucleus where – due to surface effects – the average nucleon density is below ρ_0 . This question is answered, for example, by the results of Fig. 11. This figure shows the dilepton spectra to be expected if a suitable cut on the dilepton momenta is imposed; with this cut slow vector mesons are enriched. In the realistic case shown on the right, which contains both a collision broadening and a mass shift, it is obvious that a major signal is to be expected: in the heavy nucleus *Pb* the ω -peak has completely disappeared from the spectrum. The sensitivity of such reactions is thus as large as that observed in ultrarelativistic heavy-ion reactions.

An experimental verification of this prediction would be a major step forward in our understanding of in-medium changes¹. It would obviously present a purely hadronic base-line to all data on top of which all 'fancier' explanations of the CERES effect in terms of radiation from a QGP and the such would have to live.

4 Hadron Formation

High energy photo- and electroproduction of hadrons on complex nuclei offers a promising tool to study the physics of hadron formation. The interaction of the (virtual) photon with a nucleon leads to the production of several high energy particles. Due to the soft momentum scales involved in the hadronization process the formation of the final hadrons is of nonperturbative nature and not well understood. A simple estimate for the hadron formation time can be given by the time that the constituents need to travel a hadronic radius. It should therefore be of the order of 0.5–0.8 fm/c in the rest frame of the hadron. Due to time dilatation the formation lengths of high energetic particles can reach distances in the lab frame that are of the order of the nuclear radius. Thus nuclei can serve as a kind of 'microdetector' for the determination of formation times as well as the interactions while the final

¹An experiment at JLAB is under way [47].

hadron is still being formed. Obviously, the latter is closely related to color transparency.

The HERMES collaboration [20] has investigated the multiplicities of different hadron species in deep inelastic scattering off various nuclei. Here the photon-energies are of the order of 10–20 GeV, with rather moderate $Q^2 \approx 2$ GeV². A similar experiment at somewhat smaller energies is currently performed by the CLAS collaboration at Jefferson Lab [48]. After the planned energy upgrade they will reach photon energies of the order of 2–9 GeV and similar virtualities as in the HERMES experiment.

The interpretation of the observed multiplicity spectra reach from a possible rescaling of the quark fragmentation function at finite nuclear density combined with hadron absorption in the nuclear environment [49] to purely partonic energy loss through induced gluon radiation of the struck quark propagating through the nucleus [50]. Note that a detailed understanding of energy loss and hadron attenuation in cold nuclear matter can provide a useful basis for the interpretation of jet quenching observed in ultra-relativistic heavy ion collisions at RHIC.

In our approach [51] we assume that the virtual photon interacts with the bound nucleon either directly or via one of its hadronic fluctuations. The hadronic components of the photon are thereby shadowed according to the method developed in Ref. [52] which allows for a clean-cut separation of the coherent initial state interactions of the photon and the incoherent final state interactions of the reaction products. The photon nucleon interaction leads to the excitation of one or more strings which fragment into color-neutral prehadrons due to the creation of quark antiquark pairs from the vacuum. As discussed in a recent work by Kopeliovich et al. [53] the production time of these prehadrons is very short. For simplicity we therefore set the production time to zero in our numerical realization. These prehadrons are then propagated using our semi-classical coupled-channel transport theory.

After a formation time, which we assume to be a constant τ_f in the rest-frame of the hadron, the hadronic wave function has build up and the reaction products behave like usual hadrons. During the formation time we distinguish between the so-called leading prehadrons which contain (anti-)quarks from the struck nucleon or the hadronic component of the photon and the non-leading hadrons that solely contain quarks and antiquarks created from the vacuum. The leading prehadrons can be considered as the debris of the initial hadronic state and each interacts with an effective cross section σ_{lead} during the formation time. The sum of the leading hadron cross sections

should resemble approximately that of the initial hadronic state. The non-leading prehadrons that are newly-created from the vacuum are assumed to be noninteracting during τ_f . Each time when a new hadron has formed the total effective cross section of the final state then rises like in the approach of Ref. [54].

Due to our coupled channel-treatment of the final state interactions the (pre)hadrons might not only be absorbed in the nuclear medium but can produce new particles in an interaction, thereby shifting strength from the high to the low energy part of the hadron spectrum. Our calculated multiplicity ratios of charged hadrons are shown in Fig. 12 in comparison with the experimental HERMES data [20]. The figure clearly shows that the observed hadron multiplicities can be described only with formation times $\tau_f > \approx 0.3$ fm. The curves obtained with larger formation times all lie very close together. This is a consequence of the finite size of the target nucleus: if the formation time is larger than the time needed for the preformed hadron to transverse the nucleus, then the sensitivity to the formation time is lost. In [51] we have also shown that the z -dependence on the left side exhibits some sensitivity to the interactions of the leading hadrons during the formation; the curves show in Fig. 12 are obtained with a down scaled leading hadron cross section of $\sigma_{\text{lead}} = 0.33\sigma_h$, where σ_h is the 'normal' hadronic interaction cross section.

5 Conclusions

In this lecture note we have illustrated with a few examples that photonuclear reactions can yield information that is important and relevant for an understanding of high density – high temperature phenomena in ultrarelativistic heavy-ion collisions. Special emphasis was put in this article not so much on the theoretical calculations of hadronic in-medium properties under simplified conditions, but more on the final, observable effects of any such properties. We have discussed both reactions with hadronic final states as well as those with FSI-free lepton states. While in the former reactions the FSI on the final decay products usually is strong enough to mask the in-medium spectral properties of the hadron under study, in the latter case (semi-hadronic or leptonic final states) the situation is much more encouraging. We have, for example, shown that in photonuclear reactions in the 1 - 2 GeV range the expected sensitivity of dilepton spectra to changes of

the ρ - and ω meson properties in medium is as large as that in ultrarelativistic heavy-ion collisions. We have also illustrated that the analysis of hadron production spectra in high-energy electroproduction experiments at HERMES gives information about the interaction of forming hadrons with the surrounding hadronic matter. This is important for any analysis that tries to obtain signals for a QGP by analysing high-energy jet formation in ultrarelativistic heavy-ion reactions.

Acknowledgement

This work has been supported by the Deutsche Forschungsgemeinschaft, the BMBF and GSI Darmstadt.

References

- [1] T. Ericson and W. Weise, *Pions and Nuclei*, Clarendon Press, Oxford, 1988.
- [2] H. Geissel et al., *Phys. Rev. Lett.* **88**, 122301 (2002).
- [3] J.G Messchendorp et al., *Phys. Rev. Lett.* **89**, 222302 (2002).
- [4] A. Foster et al., nucl-ex/0307018.
- [5] M.F.M. Lutz and E.E. Kolomeitsev, *Nucl. Phys.* **A700**, 193 (2002).
- [6] L. Tolos, A. Ramos, A. Polls, *Phys. Rev.* **C65**, 054907 (2002).
- [7] J.P. Wessels et al., *Quark Matter 2002 (QM 2002)*, Nantes, France, 18-24 July 2002, *Nucl. Phys.* **A715**, 262 (2003).
- [8] W. Peters et al., *Nucl. Phys.* **A632**, 109 (1998).
- [9] M. Post et al., *Nucl. Phys.* **A689**, 753 (2001).
- [10] M. Post et al., nucl-th/0309085, to be published.
- [11] J. Wambach, *Nucl. Phys.* **A715**, 422c (2003).
- [12] W. Cassing et al., *Phys.Lett.* **B363**, 35 (1995).

- [13] R. Rapp, J. Wambach, *Adv. Nucl. Phys.* **25**, 1 (2000).
- [14] R. Rapp, *Pramana* **60**, 675 (2003), hep-ph/0201101.
- [15] V. Koch et al., *Proc. Int. Workshop XXVIII on Gross Properties of Nuclei and Nuclear Excitations*, Hirschegg, Austria, Jan. 16-22, 2000, GSI Report ISSN 0720-8715.
- [16] T. Renk et al., *Phys. Rev.* **C66**, 014902 (2002).
- [17] U. Mosel, *Progr. Part. Nucl. Phys.* **42** 161 (1999)
- [18] U. Mosel, *Proc. Int. Workshop XXVIII on Gross Properties of Nuclei and Nuclear Excitations*, Hirschegg, Austria, Jan. 16-22, 2000, GSI Report ISSN 0720-8715.
- [19] M. Gyulassy et al., *Quark Gluon Plasma Vol. 3*, ed. R.C. Hwa and X.N. Wang, World Scientific, Singapore, 2003.
- [20] A. Airapetian et al., *Eur. Phys. J.* **C20**, 479; V. Muccifora et al., *Nucl. Phys.* **A711**, 254 (2002).
- [21] S. Leupold, *Phys. Rev.* **C64**, 015202 (2001).
- [22] S. Leupold, U. Mosel, *Phys. Rev.* **C58**, 2939 (1998); S. Leupold et al., *Nucl. Phys.* **A628**, 311 (1998).
- [23] S. Zschocke, O.P. Pavlenko, B. Kaempfer, hep-ph/0212201.
- [24] E.L. Bratkovskaya, *Phys. Lett.* **B529**, 26 (2002).
- [25] T. Weidmann et al., *Phys. Rev.* **C59**, 919 (1999).
- [26] M. Effenberger, E.L. Bratkovskaya, U. Mosel, *Phys. Rev.* **C60**, 044614 (1999).
- [27] W. Cassing, E.L. Bratkovskaya, *Phys. Rep.* **308**, 65 (1999).
- [28] M. Effenberger, U. Mosel, *Phys. Rev.* **C62**, 014605 (2000).
- [29] T. Falter, U. Mosel, *Phys. Rev.* **C66**, 024608 (2002).
- [30] M. Roebig-Landau et al., *Phys. Lett.* **B373**, 421 (1997).

- [31] T. Yorita et al., *Phys. Lett.* **B476** 226 (2000); H. Yamazaki et al., *Nucl. Phys.* **A670**, 202c (2000).
- [32] M. Effenberger et al., *Nucl. Phys.* **A613**, 353 (1997).
- [33] J. Lehr, M. Post, U. Mosel, *Phys. Rev.* **C68**, 044601 (2003).
- [34] P. Muehlich et al., *Phys. Rev.* **C67**, 024605 (2003).
- [35] T. Nakano et al., *Nucl. Phys.* **A684**, 71 (2001).
- [36] E. Oset, A. Ramos, *Nucl. Phys.* **A624**, 527 (1997).
- [37] T. Hatsuda, S. H. Lee, *Phys. Rev.* **C46**, 34 (1992).
- [38] F. Klingl, T. Waas, W. Weise, *Phys. Lett.* **B431**, 254 (1998).
- [39] J. Schaffner, J. Bondorf, I. N. Mishustin, *Nucl. Phys.* **A625**, 325 (1997).
- [40] P. Muehlich et al., nucl-th/0310067.
- [41] J. G. Messchendorp et al., *Eur. Phys. J.* **A11**, 95 (2001).
- [42] F. Klingl, T. Waas, W. Weise, *Nucl. Phys.* **A650**, 299 (1999).
- [43] B. Friman, *Acta Phys. Polon.* **B29**, 3195 (1998).
- [44] T. Weidmann et al., *Phys. Rev.* **C59**, 919 (1999) (1999)
- [45] G. E. Brown, M. Rho, *Phys. Rev. Lett.* **66**, 2720 (1991).
- [46] R.J. Porter et al., *Phys. Rev. Lett.* **79**, 1229 (1997).
- [47] D. Weygand, private communication.
- [48] W. K. Brooks, nucl-ex/0310032.
- [49] A. Accardi, V. Muccifora, H.-J. Pirner, *Nucl. Phys.* **A720**, 131 (2003).
- [50] E. Wang, X.-N. Wang, *Phys. Rev. Lett.* **89** 162301 (2002); F. Arleo, *Eur. Phys. J.* **C30**, 213 (2003).
- [51] T. Falter, W. Cassing, K. Gallmeister, U. Mosel, nucl-th/0303011.

- [52] T. Falter, K. Gallmeister, U. Mosel, *Phys. Rev.* **C67** 054606 (2003),
Erratum-ibid. **C68**, 019903 (2003).
- [53] B. Z. Kopeliovich, J. Nemchik, E. Predazzi, A. Hayashigaki,
hep-ph/0311220.
- [54] C. Ciofi degli Atti, B. Z. Kopeliovich, *Eur. Phys. J.* **A17**, 133 (2003).
- [55] T. Falter, U. Mosel, nucl-th/0308073.

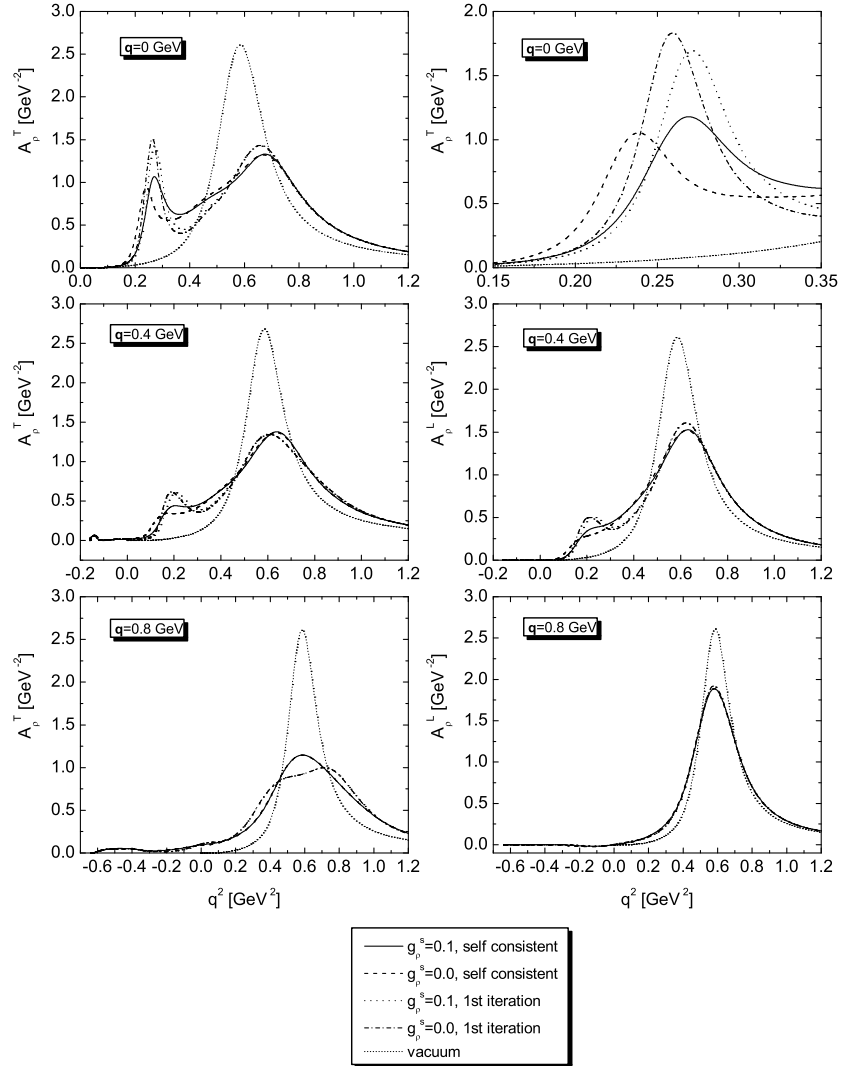


Figure 2: Spectral function of the ρ -meson at normal nuclear matter density for various momenta. Shown are the transverse and longitudinal spectral functions which are degenerate at $\vec{q} = 0$. Also shown are the effects of selfconsistency (from [10]).

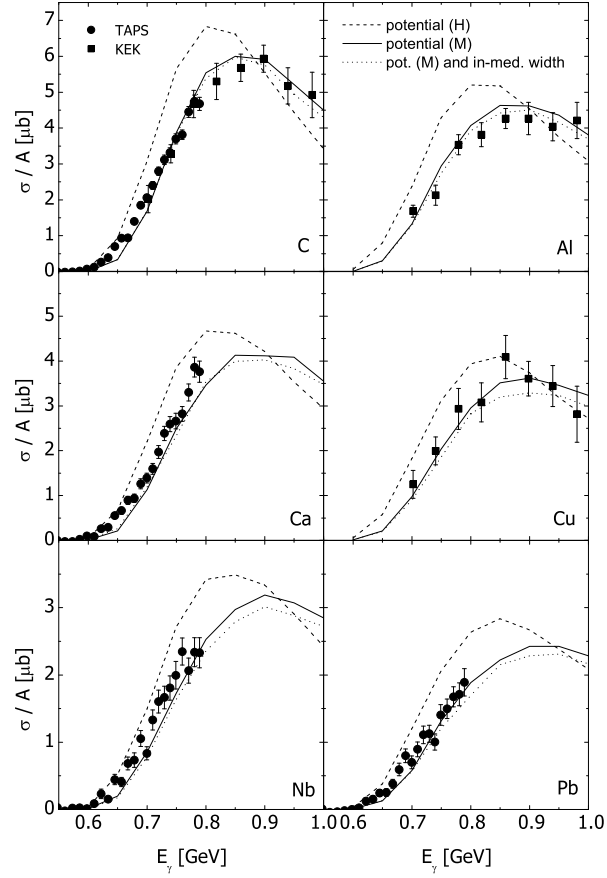


Figure 3: Results for the reaction $\gamma + A \rightarrow \eta X$. The dashed and solid lines correspond to the use of two different potentials (see text). The data are from [30] (circles) and [31] (squares) (from [33]).

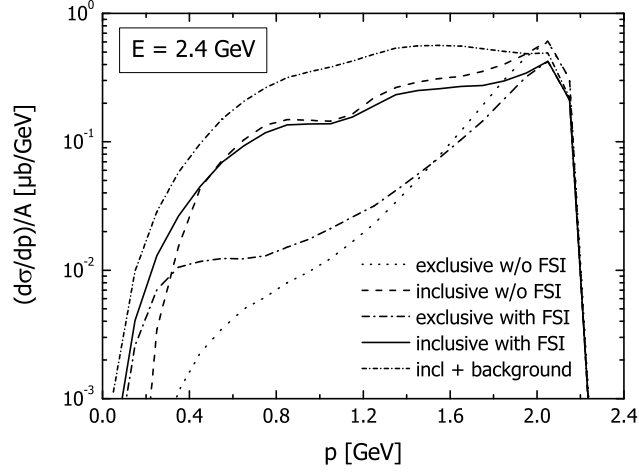


Figure 4: Momentum differential cross section for K^+K^- photoproduction off ^{40}Ca (from [34]).

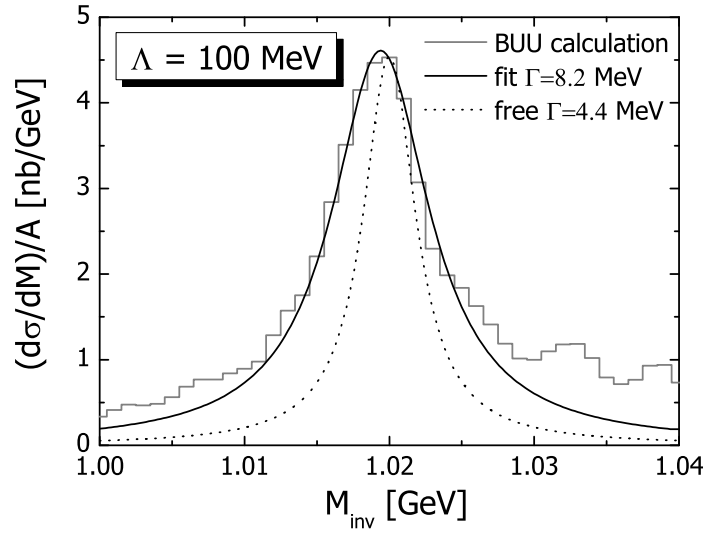


Figure 5: Mass differential cross section for K^+K^- photoproduction off ^{40}Ca with a momentum cutoff of $\Lambda = 150$ MeV at 2.4 GeV photon energy (from [34]).

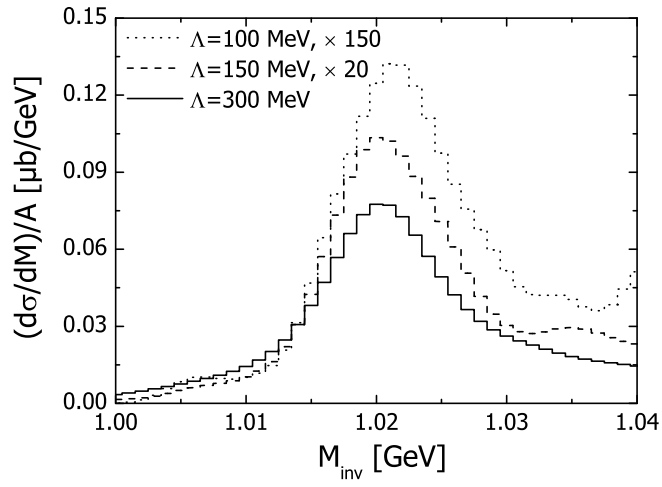


Figure 6: Mass differential cross section for K^+K^- photoproduction off ^{40}Ca at $E_\gamma = 2.4$ GeV including density-dependent mass modifications of the kaons, collisional broadening of the ϕ meson and the Coulomb potential (from [34]).

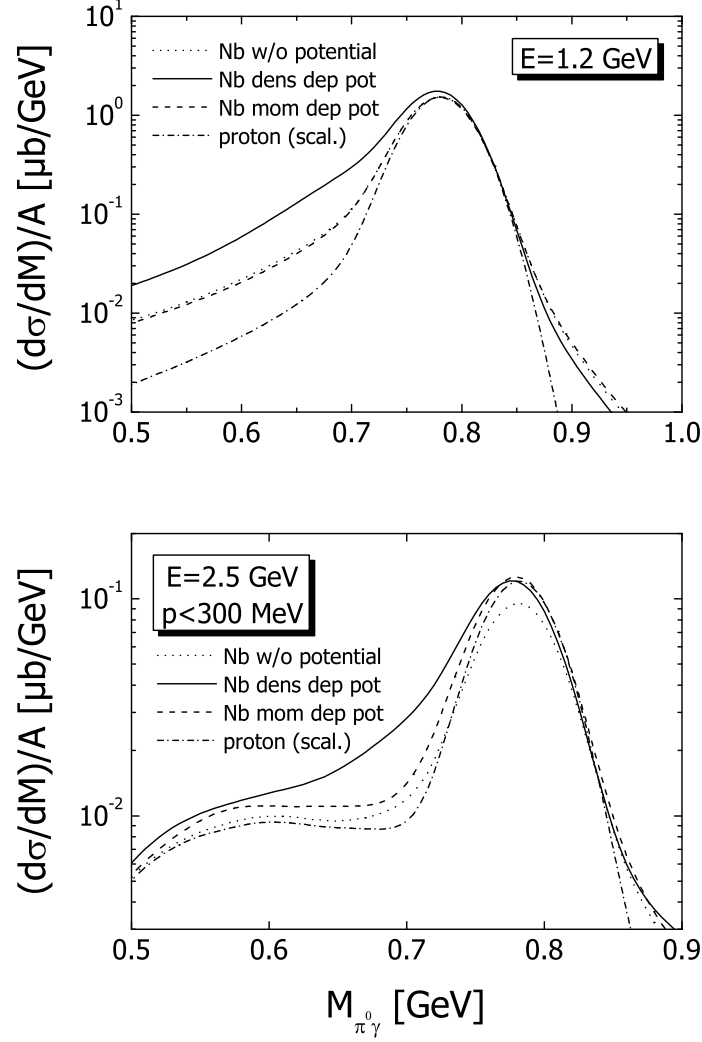


Figure 7: Mass differential cross section for $\pi^0\gamma$ photoproduction off ^{93}Nb at two different beam energies (from [40]). The results at $E_\gamma = 2.5$ GeV are obtained with a ω momentum cutoff of 300 MeV. The proton cross section is normalized to the cross section on Niobium obtained with the momentum dependent potential at the ω pole mass $m = 0.782$ GeV.

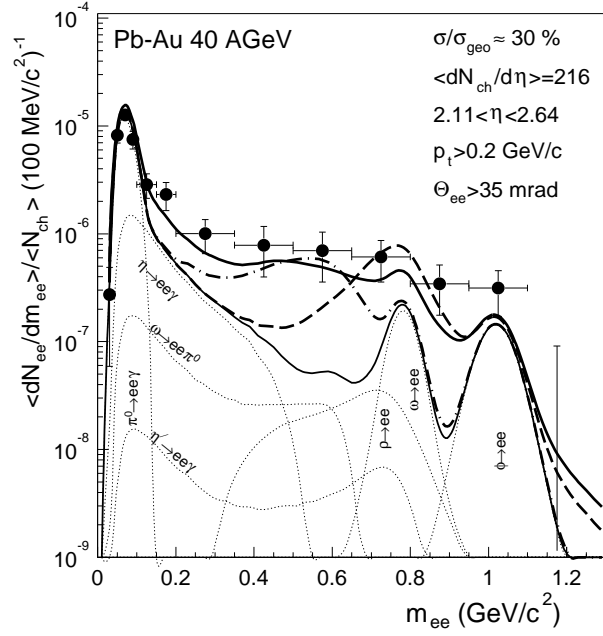


Figure 8: Invariant dilepton mass spectrum obtained with the CERES experiment in Pb + Au collisions at 40 AGeV (from [7]). The thin curves give the contributions of individual hadronic sources to the total dilepton yield, the fat solid (modified spectral function) and the dash-dotted (dropping mass only) curves give the results of calculations [14] employing an in-medium modified spectral function of the vector mesons.

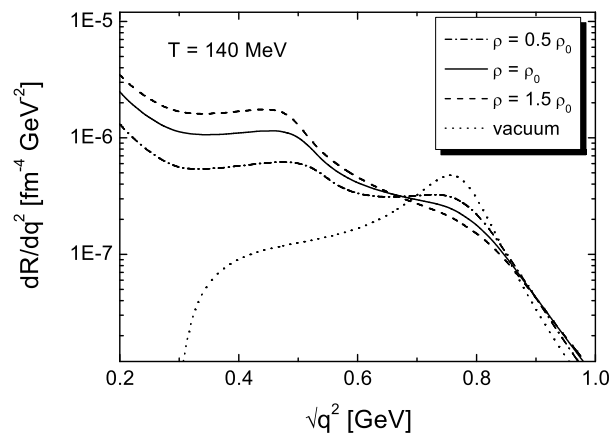


Figure 9: Momentum integrated dilepton rates at a temperature $T = 140$ MeV for three densities (from [10]).

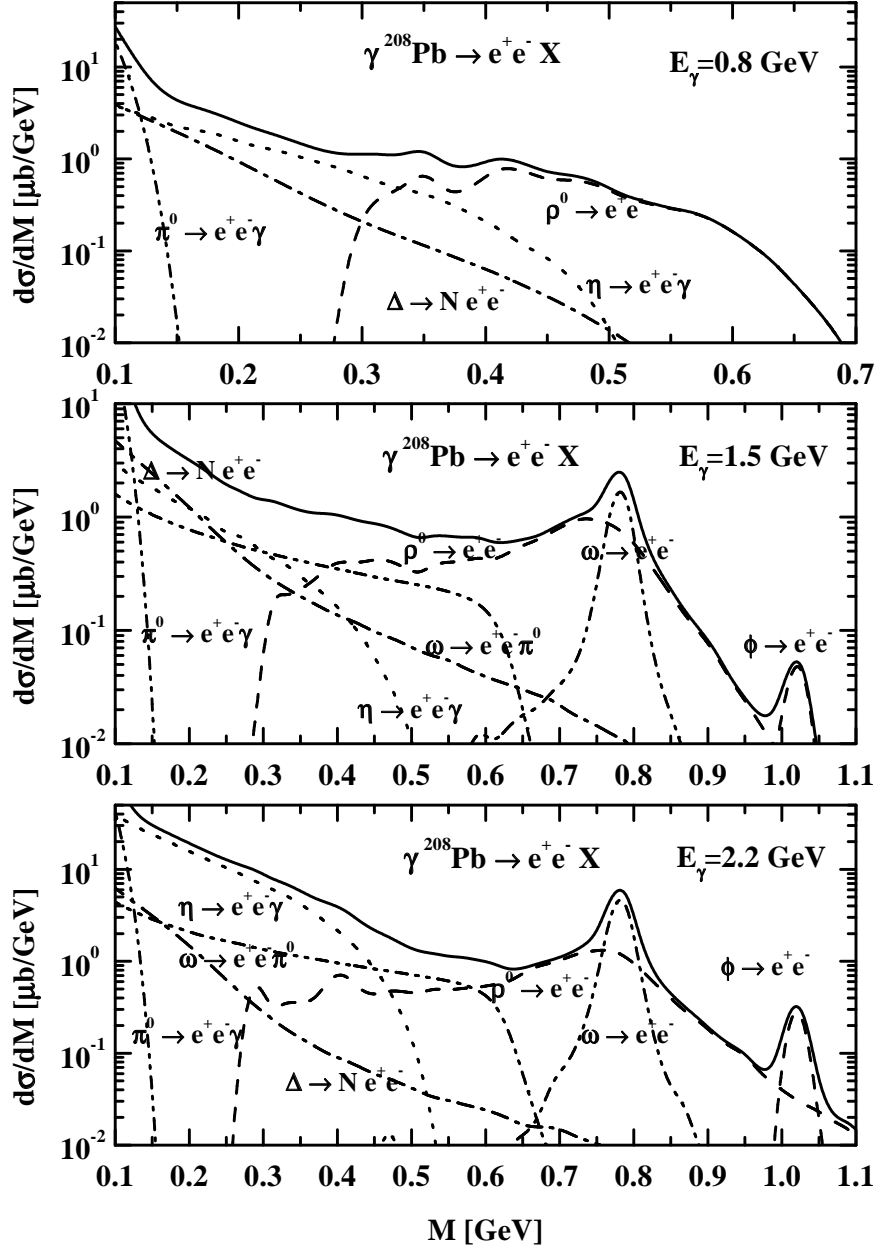


Figure 10: Hadronic contributions to dilepton invariant mass spectra for $\gamma + {}^{208}\text{Pb}$ at the three photon energies given (from [26]). Compare with Fig. 8.

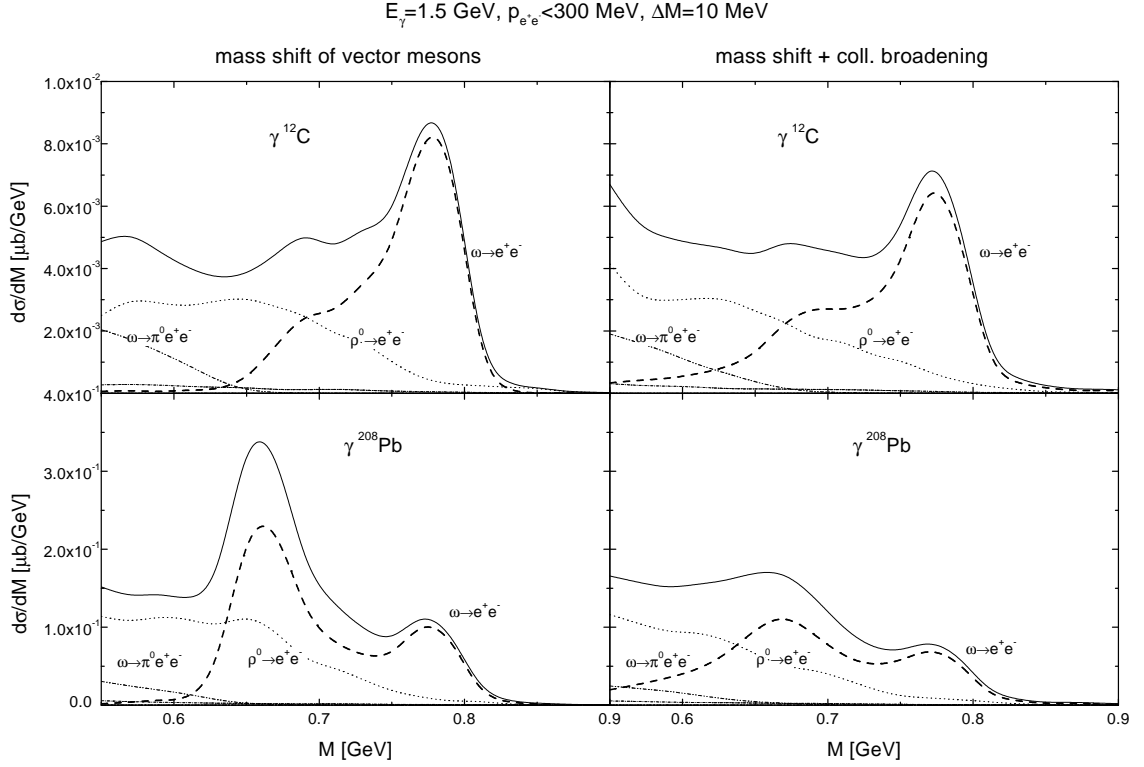


Figure 11: Dilepton mass yield with a dilepton-momentum cut of 300 MeV. Shown on the left are results of a calculation that uses only a shift of the pole mass of the vector mesons. On the right, results are given for a calculation using both mass shift and collisional broadening (from [28]).

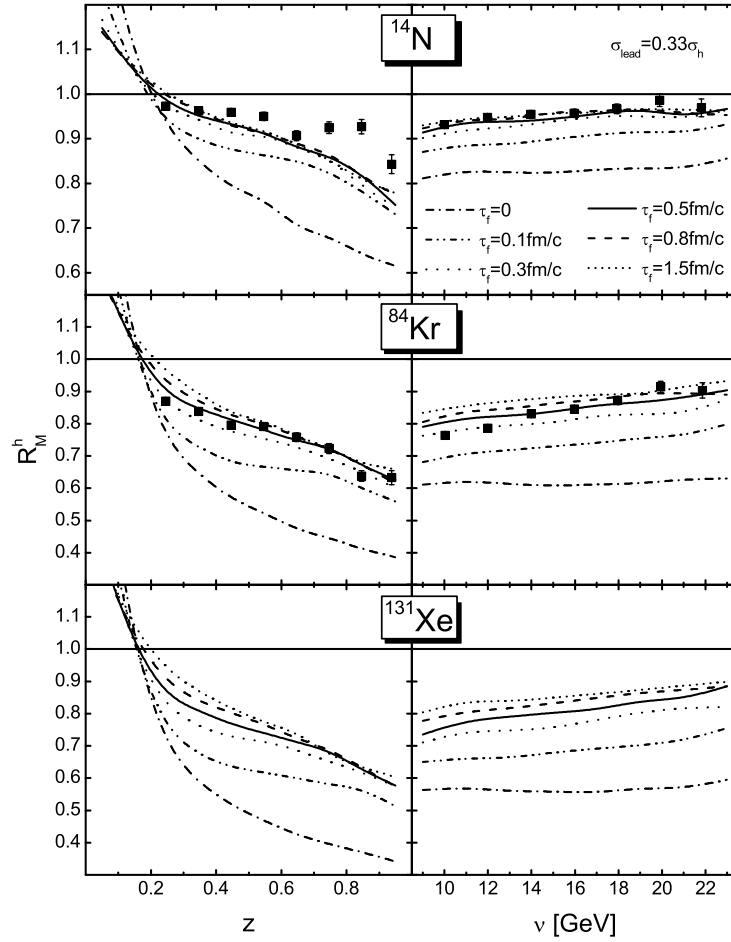


Figure 12: HERMES multiplicity of produced hadrons normalized to the deuterium as a function of photon-energy ν (right) and of the energy of the produced hadrons relative to the photon-energy, $z = E_h/\nu$. The curves are calculated for different formation times given in the figure (from [55]).